

H₂S Formation in Dark Clouds.

D. G. Navarro¹, A. Fuente¹, P. Caselli², M. Gerin³, C. Krammer⁴, E. Roueff⁵, V. Wakelam⁶, T. Alonso-Albi¹, R. Bachiller¹, S. Cazaux⁷, B. Commerçon⁸, R. Friesen⁹, S. García-Burillo¹, B. M. Giuliano², J. R. Goicoechea¹⁰, P. Gratier⁶, A. Hacar¹¹, I. Jiménez-Serra¹², J. Kirk¹³, V. Lattanzi², J. C. Loison¹⁴, P. J. Malinen¹⁵, N. Marcelino¹⁰, R. Martín-Doménech¹⁶, G. Muñoz-Caro¹², J. Pineda², M. Tafalla¹, B. Tercero¹, D. Ward-Thompson¹⁷, S. Treviño-Morales¹⁸, P. Riviére-Marichalar¹⁰, O. Roncero¹⁰ and T. Vidal⁶.

¹ Observatorio Astronómico Nacional (OAN), Alfonso XII, 3 28014, Madrid, Spain

² Centre for Astrochemical Studies, Max-Planck-Institute for Extraterrestrial Physics, Giessenbachstrasse 1, 85748, Garching, Germany

³ Observatoire de Paris, PSL Research University, CNRS, École Normale Supérieure, Sorbonne Universités, UPMC Univ. Paris 06, 75005, Paris, France

⁴ Instituto de Radioastronomía Milimétrica (IRAM), Av. Divina Pastora 7, Nucleo Central, 18012, Granada, Spain

⁵ LERMA, Observatoire de Paris, PSL Research University, CNRS, UMR8112, Place Janssen, 92190, Meudon Cedex, France

⁶ Laboratoire d'astrophysique de Bordeaux, Univ. Bordeaux, CNRS, B18N, allée Geoffroy Saint-Hilaire, 33615, Pessac, France

⁷ Faculty of Aerospace Engineering, Delft University of Technology, Delft, The Netherlands ; University of Leiden, P.O. Box 9513, NL, 2300 RA, Leiden, The Netherlands

⁸ École Normale Supérieure de Lyon, CRAL, UMR CNRS 5574, Université Lyon I, 46 Allée d'Italie, 69364, Lyon Cedex 07, France

⁹ Dunlap Institute for Astronomy & Astrophysics, University of Toronto, 50 St. George Street, Toronto, ON M5S 3H4, Canada 0000-0001-7594-8128

¹⁰ Instituto de Física Fundamental (CSIC), Calle Serrano 121, 28006, Madrid, Spain

¹¹ Laboratoire d'Astrophysique de Bordeaux, Univ. Bordeaux, CNRS, B18N, Allée Geoffroy Saint-Hilaire, 33615, Pessac, France

¹² Leiden Observatory, Leiden University, PO Box 9513, 2300-RA, Leiden, The Netherlands

¹³ Centro de Astrobiología (CSIC-INTA), Ctra. de Ajalvir, km 4, Torrejón de Ardoz, 28850, Madrid, Spain

¹⁴ Department of Physics, University of Warwick, Coventry CV4 7AL, UK

¹⁵ Institut des Sciences Moléculaires (ISM), CNRS, Univ. Bordeaux, 351 cours de la Libération, F-33400, Talence, France

¹⁶ Department of Physics, University of Helsinki, PO Box 64, 00014, Helsinki, Finland; Institute of Physics I, University of Cologne, Cologne, Germany

¹⁷ Harvard-Smithsonian Center for Astrophysics, Cambridge, MA 02138, USA

¹⁸ Jeremiah Horrocks Institute, University of Central Lancashire, Preston PR1 2HE, UK

¹⁹ Chalmers University of Technology, Onsala Space Observatory, 439 92 Onsala, Sweden.

Abstract

Sulfur is of fundamental importance in a wide variety of phenomena such as life on Earth. This element is one of the most abundant elements in space $S/H \sim 1.3 \times 10^{-5}$, but sulfurated molecules are not as abundant as expected, thus a better understanding of sulfur chemistry is needed. We study and model the abundance of H_2S in two prototypical dark clouds, TMC1 and Barnard 1, to shed light on the physical and chemical processes involved in H_2S creation and destruction. Our observations are consistent with a PDR model in which H_2S is formed in grain mantles and released to gas phase via photodesorption. We cannot discard the contribution of other desorption processes, such as chemical desorption and/or grain-grain collisions, to enhance the H_2S abundance.

1 Introduction

Astrochemistry is an important tool to characterize the evolution of molecular gas from diffuse clouds to dense cores. In this dynamical evolution, gas cooling and gas ionization degree regulate cloud collapse. Sulfur plays an important role in this collapse since it is one of the most abundant elements in the universe, with a relative abundance of $S/H \sim 1.3 \times 10^{-5}$ [1], and it is the main donor of electrons in the 3.7 - 7 magnitude range. Despite its high relative abundance, sulfurated compounds are not as abundant as expected in molecular clouds. Sulfur is thought to be depleted by a factor of 10^3 inside dark clouds compared to its cosmic abundance. The missing sulfur might be locked into grain mantles (e.g. [18]), which would form H_2S preferentially due to the high hydrogen abundance and mobility in the ice matrix. Therefore, studying the abundance of the H_2S molecule, which cannot be explained solely by gas-phase chemical reactions [24], may shed light into the physical and chemical processes responsible for sulfur depletion. We investigate the H_2S gas-phase abundance in two prototypical dark clouds: TMC1 and Barnard 1.

2 TMC1 and Barnard 1

TMC1, part of the Taurus molecular cloud (TMC), is one prototypical filamentary dark cloud cold core with quiescent star forming regions, at 140 pc. One of the largest Planck Galactic Cold Clumps (PGCC) groups in TMC is the Heiles Cloud 2 [13][20][22]. Malinen et al [17] identified two long filaments in HCL 2 at the eastern edge of the Taurus Molecular Ring, based on near-IR (NIR) extinction and Herschel data; one of these filaments was TMC-1. There are three visual extinction peaks along the TMC-1 filament, the well-known positions TMC1-CP, TMC1-C2 and TMC1-NH3 (see Fig. 1).

Barnard 1, embedded in the western sector of the 30pc wide molecular cloud complex Perseus, is a close (230pc) and young, intermediate-mass star forming cloud. It is known to host class 0 protostars [11][12], providing a bridge between the low-mass star formation of Taurus, and the massive star forming regions such as the Orion molecular cloud. This core

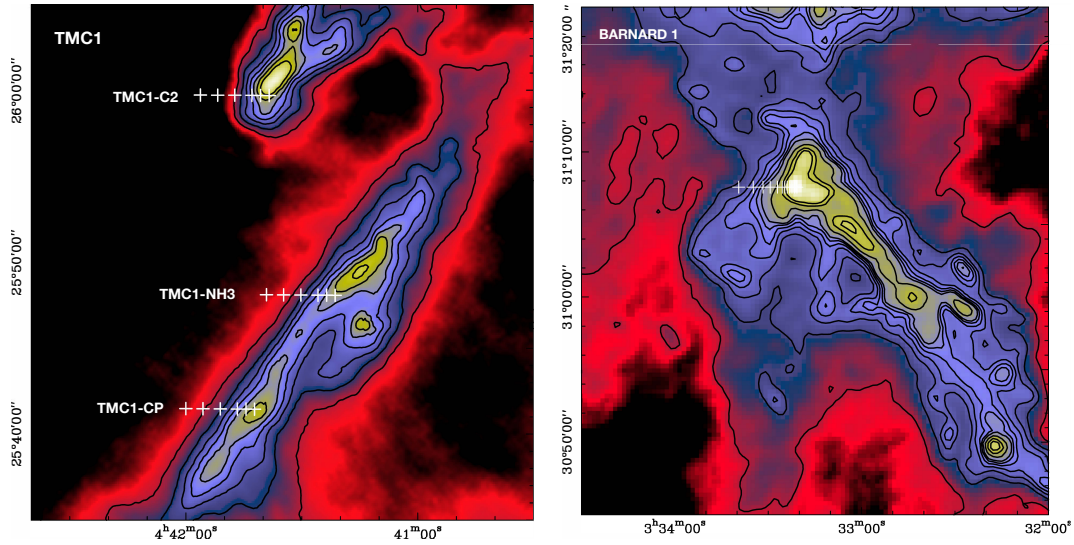


Figure 1: Visual extinction maps of TMC1 and Barnard 1 filaments, respectively (Kirk et al., in prep, Zari et al. 2015). White crosses mark the observed positions.

hosts two candidates for a first hydrostatic core [8], B1b-N and B1b-S, proving its young star formation. We observed through a cut associated with the extinction peak in B1b (see white marks in Fig. 1), which is the most prominent core in B1.

3 IRAM 30m and Yebes 40m telescopes

This work is based on data from the GEMS IRAM 30m Large Program (Gas phase Elemental abundances in Molecular CloudS, PI: A. Fuente) and complementary observations carried out with the Yebes 40m telescope. Using the wide bandwidth of the IRAM 30m receivers, we can observe the most intense 3mm and 2mm lines of these species with only 4 receiver setups. As backends we used the Fast Fourier Transform spectrometers (FFTS) correlators, which provide a frequency resolution of ~ 49 kHz, enough to resolve the narrow lines expected in this dark cloud. The Yebes 40m telescope is equipped with HEMT receivers for the 2.2-50 GHz range, and a SIS receiver for the 85-116 GHz range. Single-dish observations in K-band (21-25 GHz) and Q-band (41-50 GHz) can be performed simultaneously. The intensity scale is T_{MB} and calibration errors are $\sim 20\%$.

4 H₂S abundances

The analysis of the $J = 1 \rightarrow 0$, $J = 2 \rightarrow 1$ and $J = 3 \rightarrow 2$ lines of CS and its isotopologues allows us to derive reliable values of line opacities and hydrogen densities towards the considered regions. We use Markov Chain Montecarlo sampling methods [5] as described in [7], and the radiative transfer code RADEX [23] to estimate the physical conditions of the gas. To estimate

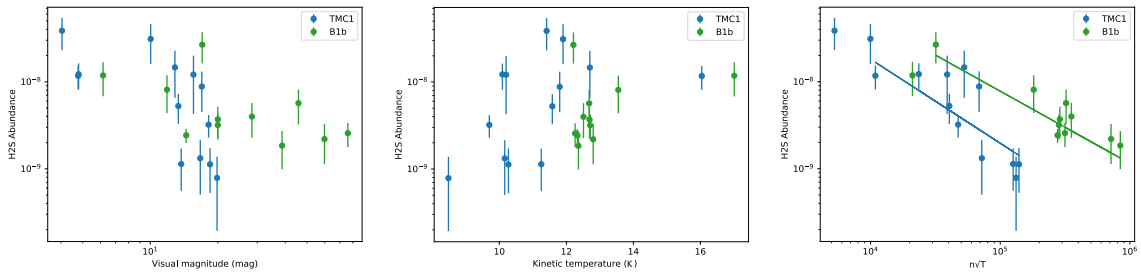


Figure 2: H₂S abundance against visual magnitude, kinetic temperature, and $n\sqrt{T}$ respectively, to show the dependence in eq. (1), for TMC1 (blue) and Barnard 1 (green).

the ortho-H₂S abundances we have used the code RADEX and the collisional coefficients for ortho-H₂O [4], assuming thermal ortho-para ratio for H₂ and scaled to ortho-H₂S. We hence fit the line intensities of the o-H₂S $J = 1_{1,0} \rightarrow 1_{0,1}$ line assuming the physical conditions derived from CS observations. The H₂S abundance is calculated assuming an ortho-to-para ratio of 3. Fig. 2 shows the H₂S abundances as a function of the visual extinction in TMC 1 and Barnard 1b. The H₂S gas-phase abundance reaches its maximum value, $X(\text{H}_2\text{S}) \sim 1 - 3 \times 10^{-8}$, at the edges of the clouds. For visual extinctions larger than ~ 10 mag, the abundance steeply decreases until values of \sim a few 10^{-10} at $A_V \sim 20$ mag. For dust grain temperatures below the H₂S evaporation temperature, ~ 50 K [16], the H₂S molecules are expected to stick on grains in every collision and the depletion time scale is given by

$$X(\text{H}_2\text{S}) \propto t_{\text{st}} \equiv \frac{1}{n_{\text{gr}} \sigma_{\text{gr}} v_0} \propto \frac{1}{n\sqrt{T}}. \quad (1)$$

Fig. 2 shows the derived H₂S abundances as a function of the gas kinetic temperature and the parameter, $n\sqrt{T}$. Towards both sources, the H₂S abundance decreases as $\sim \frac{1}{n\sqrt{T}}$, which corresponds to the slope of -1 seen in Fig. 2c, as expected when molecular freeze-out on grain surfaces is the main destruction mechanism. The scattering in the estimated values of the H₂S abundances is, however, large. Besides, the H₂S abundances estimated towards Barnard 1-b seems to be systematically higher than those towards TMC 1 by a factor of ~ 3 .

5 Chemical model

One interesting issue is to compare the sulfur and oxygen chemistry. Similarly to H₂O, H₂S cannot be efficiently formed in gas phase in dark clouds. The observed abundances of H₂S should be the consequence of the desorption of H₂S molecules from the grain surfaces. The physical conditions in dark clouds greatly constrain the possible desorption mechanisms: thermal desorption is only feasible for grain temperatures greater than 50 K [16], and sputtering is important in fast shocks ($v_s > 5$ km s⁻¹), requiring our line profiles to be much wider. In a first approximation, we can consider that photodesorption by UV field and secondary photons are the main desorption agents. We have adapted the analytical model proposed for H₂O by

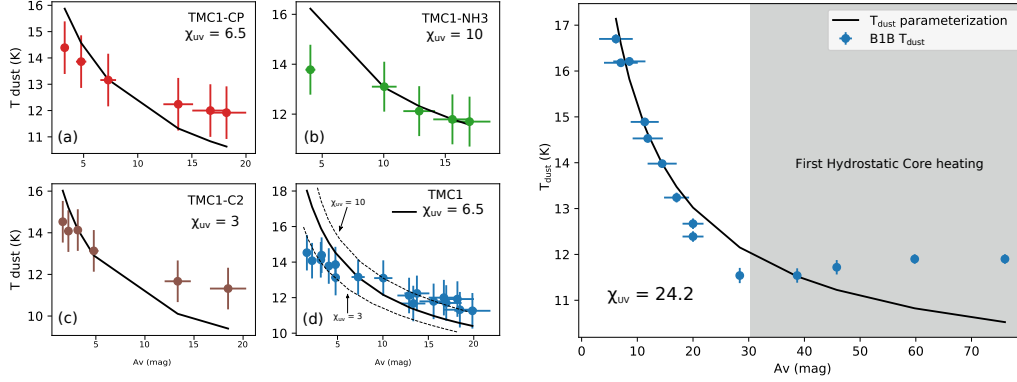


Figure 3: Fits of the dust temperature vs A_V for the three cuts in TMC 1 and the one in Barnard-1b, according to [14] parameterization. The best fit value of the incident UV field is $\chi_{UV} \sim 6.5$ for TMC 1 and $\chi_{UV} \sim 24$ for Barnard-1b, in units of the Draine field.

[15] to the case of H_2S molecule. In this model, the grains are supposed to be covered by an ice layer and photodesorption is the only H_2S formation path. On the other hand, freezing onto grain mantles and photodissociation are responsible for gas-phase H_2S destruction. We assume that secondary photons do not contribute to the photodissociation rate R_{H_2S} , and their extinction is similar to that of the FUV radiation. In the stationary state, creation (lhs of (2)) and destruction rates (rhs of (2)) are equal, and therefore:

$$(G_0 F_0 e^{-1.8A_V} + \Phi_{SP}) Y_{H_2S} f_{s,H_2S} n_{gr} \sigma_{gr} = G_0 R_{H_2S} e^{-1.7A_V} n(H_2S) + n(H_2S) v_0 n_{gr} \sigma_{gr}, \quad (2)$$

where $Y_{H_2S} = 1.2 \times 10^{-3}$ molecules per incident photon is the photo-desorption yield of H_2S [6], f_{s,H_2S} is the fraction of desorption sites occupied by H_2S ice, G_0 is the Habing field ($G_0 = 1.7\chi_{UV}$), F_0 is the flux of UV photons, and Φ_{SP} is the rate of secondary photons produced by cosmic rays interacting with H_2 [9]. Rearranging:

$$x(H_2S) = \frac{(G_0 F_0 e^{-1.8A_V} + \Phi_{SP}) Y_{H_2S} f_{s,H_2S} \sigma_H}{G_0 R_{H_2S} e^{-1.7A_V} + v_0 n_H(A_V) \sigma_H} \quad (3)$$

In addition, we equate the sticking rate of S atoms to the desorption rate of H_2S to get the analytic expression for the fraction of sites covered by H_2S :

$$f_{S,H_2S} = \frac{n(S) v_0}{Y(G_0 F_0 e^{-1.8A_V} + \Phi_{SP})} \quad (4)$$

Equations (3) and (4) determine the H_2S abundance for given values of A_V and n . Now, we discuss the general properties of the model before going into detail on the selected sources. When the visual magnitude increases, f_{S,H_2S} in Eq. (4) increases as well, reaching a saturation value. The abundance relative to water found in comets is of the order of 2% [2], thus we take the saturation value as $f_{S,H_2S,max} = 0.02$. In the low visual magnitude and density regime, both gas-phase H_2S formation and destruction processes are proportional to G_0 . As a consequence, the gas-phase H_2S abundance should reach an equal value, independently of G_0 .

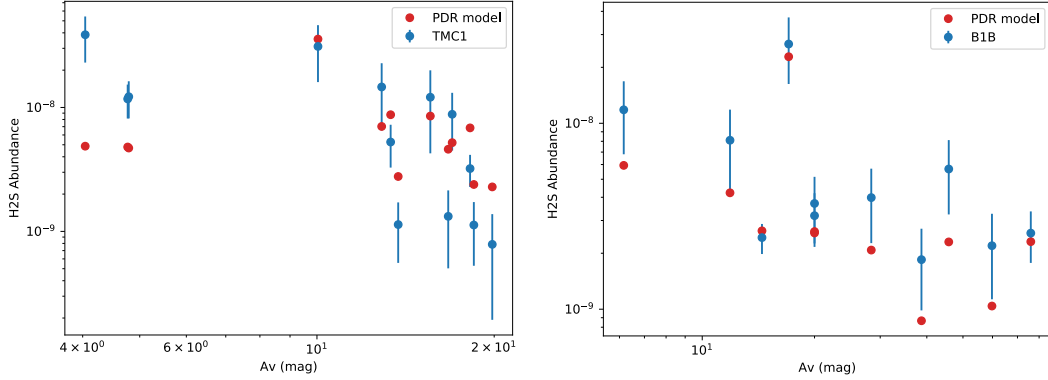


Figure 4: H₂S abundance (blue) and the model prediction (red) for TMC1 and Barnard 1, assuming a secondary photon flux of $\Phi_{\text{SP}} = 2 \times 10^4$ photons cm⁻² s⁻¹ and $\Phi_{\text{SP}} = 4 \times 10^4$ photons cm⁻² s⁻¹, respectively.

Once saturation occurs, $X(\text{H}_2\text{S})$ in Eq. (3) starts dropping due to the increasing density, and therefore depletion onto grains. In the shielded regime, the flux of secondary photons, Φ_{SP} and the gas density determine the H₂S abundance, Values of Φ_{SP} between 750 and a few 10⁴ photon cm⁻² s⁻¹ have been reported in the literature [10][21]. We let Φ_{SP} to vary within this range.

6 Comparison with observations

In order to compare our model with the TMC 1 and Barnard 1b observations, the incident radiation field needs to be quantified. This is done using the parametric expression that relates dust temperature, visual magnitude, and Draine field reported by [14]. We obtain the best fit with incident UV field of $\chi_{UV} \sim 6.5$ for TMC 1 and $\chi_{UV} \sim 24$ for Barnard-1b, in units of the Draine field (see Fig. 3). We have introduced these numbers in equations (3) and (4) to fit the H₂S abundances and obtain a reasonable fitting of the observed H₂S abundances with $\Phi_{\text{SP}} = 2 \times 10^4$ photons cm⁻² s⁻¹ in TMC 1 and $\Phi_{\text{SP}} = 4 \times 10^4$ photons cm⁻² s⁻¹ in Barnard 1b (see Fig. 4). Within this scenario, the difference between the measured H₂S abundance between TMC 1 and Barnard 1b is due to a different cosmic ray ionization rate. A more detailed and complete chemical modeling of the two targets is required to confirm this hypothesis. First of all, we need to take into account the 3D physical structure of the cores in order to derive a precise H₂S abundance profile. Recent laboratory work suggests that chemical desorption might be important for H₂S [19]. To introduce chemical desorption in the model would allow to explain the H₂S abundance in the shielded cloud with a lower secondary photons flux. Our simple model considers adsorption and desorption processes but does not account for surface chemistry and thus neglects the influence that the grain temperature is expected to have in the H₂S formation rate. Moreover, although fast shocks are not occurring in these dense clouds, [3] suggests that sputtering by grain-grain collisions could be efficient to desorb molecules at low velocities, hence increasing the H₂S abundance.

7 Conclusions

Single-dish observations of two nearby dark clouds, TMC1 (140 pc) and Barnard 1 (235 pc) are used to investigate the chemistry of H₂S in starless cores. We have found that the H₂S abundance presents its maximum abundance at the cloud edge, $X(\text{H}_2\text{S}) \sim 1 - 3 \times 10^{-8}$ and decrease with density towards the visual extinction peaks. To explain this behavior we propose a simple chemical model which assumes that H₂S is formed on grain mantles, and released into gas via photodesorption. Even though this model is quite simple, we find a general agreement with the observations which supports that hydrogenation of S atoms on the grain surfaces is the main formation path for H₂S.

Acknowledgments

We thank the Spanish MINECO for funding support from AYA2016-75066-C2-1/2-P, and ERC under ERC-2013-SyG, G. A. 610256 NANOCOSMOS. JM acknowledges the support of ERC-2015-STG No. 679852 RADFEEDBACK. SPTM and JK acknowledges to the European Union's Horizon 2020 research and innovation program for funding support given under grant agreement No 639459 (PROMISE).

References

- [1] M. Asplund, N. Grevesse, A.J. Sauval, P. Scott, *Ann. Rev. Astron. Astrophys.* 47, 481 (2009)
- [2] D. Bockelée-Morvan, N. Biver, 2017 *Phil. Trans. R. Soc. A* 375: 20160252
- [3] P. Caselli, T.W. Hartquist and O. Havnes, *A&A* 322, 296–301 (1997)
- [4] M.L. Dubernet, F. Daniel, A. Grosjean and C.Y. Lin, *A&A* 497, 911–925 (2009)
- [5] D. Foreman-Mackey, D. W. Hogg, D. Lang, J. Goodman, 2013 *PASP* 125, 306
- [6] A. Fuente et al, 2017 *ApJL* 851 L49
- [7] A. Fuente et al. arXiv:1809.04978 [astro-ph.GA]
- [8] M. Gerin et al. *A&A*, 606 (2017) A35
- [9] R. Gredel, S. Lepp and A. Dalgarno, *ApJ* 347:289-293, 1989
- [10] T.W. Hartquist and D.A. Williams, 1990 *MNRAS* 247, 343
- [11] J. Hatchell, J. S. Richer, G. A. Fuller et al. 2005, *A&A*, 440, 151
- [12] J. Hatchell, G. A. Fuller, J. S. Richer, 2007, *A&A*, 472, 187
- [13] E. C. Heiles, *Astrophys. J.*, 1968, vol. 151
- [14] S. Hocuk, L. Szűcs, P. Caselli, S. Cazaux, M. Spaans and G. B. Esplugues, *A&A* 604, A58 (2017)
- [15] D. Hollenbach, M. J. Kaufman, E. A. Bergin, and G. J. Melnick, *ApJ* 690 1497
- [16] A. Jiménez-Escobar and G. M. Muñoz Caro, *A&A* 536, A91 (2011)
- [17] J. Malinen et al. *A&A*, 544 (2012) A50
- [18] T. J. Millar, E. Herbst, 1990, *A&A*, 231, 466

- [19] Y. Oba, T. Tomaru, T. Lamberts, A. Kouchi and N. Watanabe, *Nat. Astron.* 2 (2018) 228
- [20] T. Onishi, A. Mizuno, A. Kawamura, H. Ogawa & Y. Fukui, 1996, *ApJ*, 465,815
- [21] C. J. Shen, J. M. Greenberg, W. A. Schutte and E. F. van Dishoeck, *A&A* 415, 203-215 (2004)
- [22] L. V. Tóth, M. Haas, D. Lemke, K. Mattila and T. Onishi, *A&A*, 420 2 (2004) 533-546
- [23] F.F.S. Van der Tak et al, 2007, *A&A* 468, 627-635
- [24] V. Wakelam, P. Caselli, C. Ceccarelli, E. Herbst, & A. Castets, 2004a, *A&A*, 422, 159